

# Spectral monitoring of NGC 4151 and 3C390.3 at the 6 m telescope

A.I. Shapovalova<sup>a</sup>, A.N. Burenkov<sup>a</sup>, N.G. Bochkarev<sup>b</sup>

<sup>a</sup> Special Astrophysical Observatory of the Russian AS, Nizhnij Arkhyz 357147, Russia

<sup>b</sup> Special Astrophysical Observatory of the Russian AS, Nizhnij Arkhyz 357147, Russia

<sup>c</sup> Sternberg Astronomical Institute, Moscow, Russia, 119899

Received June 17, 1996; accepted June 30, 1996.

## Abstract.

The results of spectral monitoring of the Seyfert galaxies NGC 4151 (1986–96) and 3C390.0 (1995–96) obtained at the 6 m telescope are presented. The behaviour of the broad component profiles of  $H_\beta$  and continuum is studied. Quasisimultaneous variations of the fluxes in the blue and red wings of  $H_\beta$  in both galaxies are detected, which is indicative of the absence of considerable radial motions in BLR. It is shown that in 3C390.3 spectra the variability of the blue wing of  $H_\beta$  from November 1995 to February 1996 was twice as intensive as that of the red one. We confirm the obtained by Veilleux and Zheng (1991) sinusoidal dependence with a period of  $\sim 10$  years for the ratios of the observed fluxes of the blue and red wings of  $H_\beta$  in 3C390.3 spectra. The observed  $H_\beta$  line profiles of this galaxy can be explained by the models of inhomogeneous line-emitting disk or biconical BLR.

**Key words:** Seyfert galaxies: individual: NGC 4151, 3C390.3 — broad emission lines — spectral variability

## 1. Introduction

Nucleus variability of most Seyfert galaxies in both broad emission lines and in continuum is a unique feature for studying interiors of AGN.

Multiwave spectral monitoring carried out in the last years of some Seyfert galaxies according to the international “AGN Watch” program has made a revolution in our insight into physical characteristics of BLR. These observations allowed reliable ascertainment of the time-delayed response of emission lines to continuum variations (echograms of BLR). Reliable evidence has been obtained up to now of stratification of matter ionization degree with distances from the centre: highly ionized gas responds to the variations of energy output from the continuum central source sooner than the low-ionized gas, i.e. these regions are located at different distance from the center. However, kinematics of line emitting clouds is not well studied, since for this to be done it is necessary to have spectra obtained with a high photometric accuracy (a few per cent) and a good spectral resolution (1–5 Å). Theoretical calculations of Bochkarev and Antokhin (1982) have shown that in the medium of optically thick clouds one can recognize kinematic models of BLR by profile variations of broad emission lines, including the cases of matter inflow and

outflow, motion with acceleration or deceleration, etc. Since 1986 we carry out spectral monitoring of several SyG with the 6 m telescope of SAO RAS to study the structure and kinematics of BLR. In 1986–96 we obtained about 400 spectra of SyGs — NGC 3516, 4151, 5548, 7469 and 3C390.3. Here we present the observational results for NGC 4151 (1986–96) and 3C390.3 (1995–96).

## 2. Observations

Spectra of NGC 4151 and 3C390.3 nuclei are obtained with the 6 m telescope of the Special Astrophysical Observatory (N.Arkhyz — North Caucasus) in the Nasmyth focus using the spectrograph SP124 + TV scanner with a resolution of 3–4 Å and S/N = 20 in the wavelengths 4000–5000 Å (1986–94), and in the prime focus of the 6 m telescope with a multi-pupil field spectrograph (MPFS) + CCD (resolution 4 Å), or with the spectrograph UAGS (a long slit mode) + CCD (resolution 5–10 Å), S/N = 50 – 100 (1994–96).

The spectra were scaled to one and the same flux by the emission line [OIII] 4959 for NGC 4151 and [OIII]5007+[OIII]4959 lines for 3C390.3 under the assumption that the flux in this line was unaffected during the observational run. The spectra of NGC 4151, obtained with the scanner in 1986–90, did not gener-

ally include the [OIII] line, and so they were scaled by the narrow component of the HeII 4686 emission line, correlated to [OIII] 4959 by individual spectra of 1986–96. In the period of monitoring I[OIII]/I(HeII–narrow) ratio was constant within the accuracy of our measurements (5%–10%).

### 3. Results

#### 3.1. NGC 4151

In 1986–95 about 150 spectra of the NGC 4151 nucleus were obtained at the 6 m telescope scanner with an aperture of 2". Generally two spectra were taken on each night at the left and right strobes of the scanner in order to correct for possible defects. Then the spectra taken on one and the same night were summed up and only the summary spectra were analyzed. If the spectra taken on the nights following each other coincided, then their sums were analyzed to increase photometric accuracy. For individual spectra within the spectral range 4700–4800 ÅÅ the S/N was usually about 20, while for the summarized spectra the S/N was of the order of 30–50. A total of more than 60 scanner spectra were analyzed, part of which correspond to the average over several nights.

Besides, in 1994–96 the spectra of NGC 4151 were obtained with a long slit (UAGS + CCD) or (MPFS + CCD) with S/N = 50–100 (17.05.94, 18.05.94; 23.04.95, 26.05.95; 11.01.96, 11.02.96, 12.02.96). These spectra were integrated in the aperture (2–3)" × 4". The spectra taken with the scanner and with a long slit on close dates almost coincided.

Emission spectra obtained after continuum subtraction were analyzed. Measurements of the broad component of  $H_\beta$  were made after subtraction of the narrow component.

##### a) Broad component variability of $H_\beta$ and continuum

Fig. 1 shows the average profiles of  $H_\beta$  for the epoch of minimum (spring 1987) and maximum (spring 1995). The observed integral fluxes of the broad component of  $H_\beta$  for these epochs differ by a factor of 8.

The average profiles of  $H_\beta$  obtained in different years are presented in Figs. 2–3. It is well seen that in 1986–91 the maximum amplitude of the red wing of  $H_\beta$  was lower than that of the blue wing (Figs. 2–3); in 1993–95 the wings were of nearly equal brightness, whereas in 1996 the red wing was brighter than the blue one (Fig. 4). The continuum flux intensity was measured within 4705–4765 ÅÅ. The observed integral intensity of different components of  $H_\beta$  emission line was determined in the following wavelength intervals:

- the total broad component — 4795–4930; the blue wing — 4795–4857 ÅÅ (corresponds to

$V \leq -1200$  km/s relative to the narrow component of  $H_\beta$ );

- the red wing — 4857–4930 ÅÅ (includes the central component of the broad  $H_\beta$ , Red\_all in Figs. 6–11);

- and 4897–4930 ÅÅ (only the wing with  $V \geq 1200$  km/s, Red\_low in Figs. 6–11).

All the intervals, except the last one, are the same as those adopted by Maoz et al. (1991) in the analysis of the broad component of  $H_\beta$  from the 1987–88 monitoring.

Fig. 5 shows the integral fluxes of the broad component of  $H_\beta$  and continuum during the whole monitoring period (1986–96). On the average the fluxes in lines and continuum increased 5–6 times from 1986 to 1996. In some years the intensities of the broad component and continuum varied during several days by a factor of 1.5–2, and on a time scale of 1–3 months (monitoring interval with a maximum frequency) — by a factor of 1.5–3.

##### b) Velocity field

The S/N ratio in the wings of the broad component of  $H_\beta$  is high enough to study the behaviour of the blue and red wings separately. This may throw light on the velocity field in BLR of this galaxy. The observed integral fluxes in the blue and red wings of  $H_\beta$  from monitoring results obtained in different years are shown in Figs. 6–10.

Fig. 11 gives the averaged fluxes in the wings for every year. It is well seen that the integral fluxes in the blue and red wings of  $H_\beta$  vary in phase without any lag. Quasisimultaneous flux variations in the wings of  $H_\alpha$  and  $H_\beta$  were obtained also by Maoz et al. (1991) from the results of NGC 4151 monitoring in 1987–88. Our data confirm these results on a time scale of 10 years. According to the model calculations of Maoz et al. (1991) in the case of radial motions there must be a lag of the order of 11 days in the wing responses relative to each other. Thus, our results rule out considerable radial motions (inflow or outflow) in BLR NGC 4151. Fig. 12 presents integral flux ratios in the blue and red wings of  $H_\beta$  at the moment of monitoring, and the average values for every year are given in Fig. 13. From these data one may suspect a periodicity of 2–3 years (1986–92) in the flux variations of the blue and red wings, and a periodicity of an attenuating amplitude in 1994–95.

#### 3.2. 3C 390.3

Optical spectra of 3C390.3 were taken at the 6 m telescope as part of an ongoing IAU monitoring program of variability of active galactic nuclei ("Watch AGN"). 3C390.3 is the first radio emitting AGN for which IAU monitoring is being carried out (1995–96). The spectra of 3C390.3 were obtained at the 6 m tele-

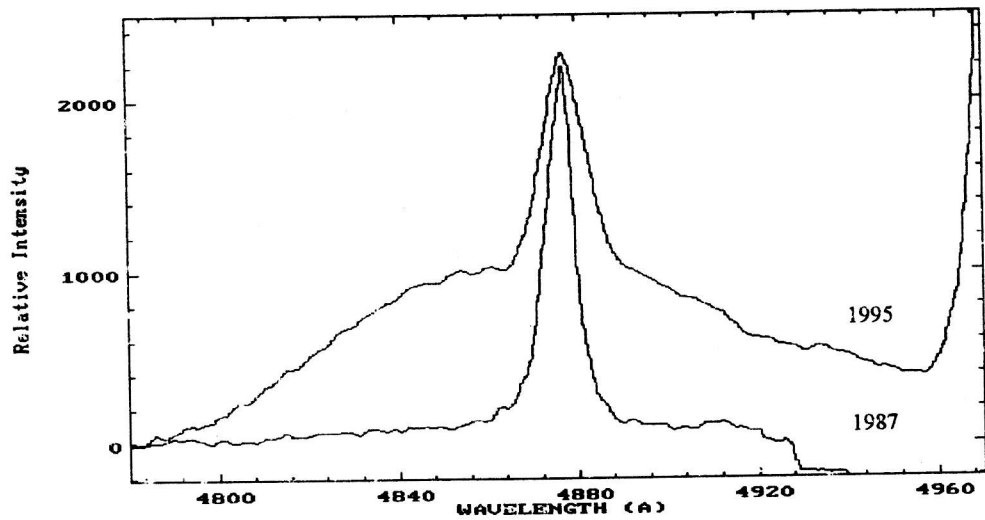


Figure 1: NGC 4151. Average profiles of broad  $H_{\beta}$  for each year (epoch of minimum and maximum)

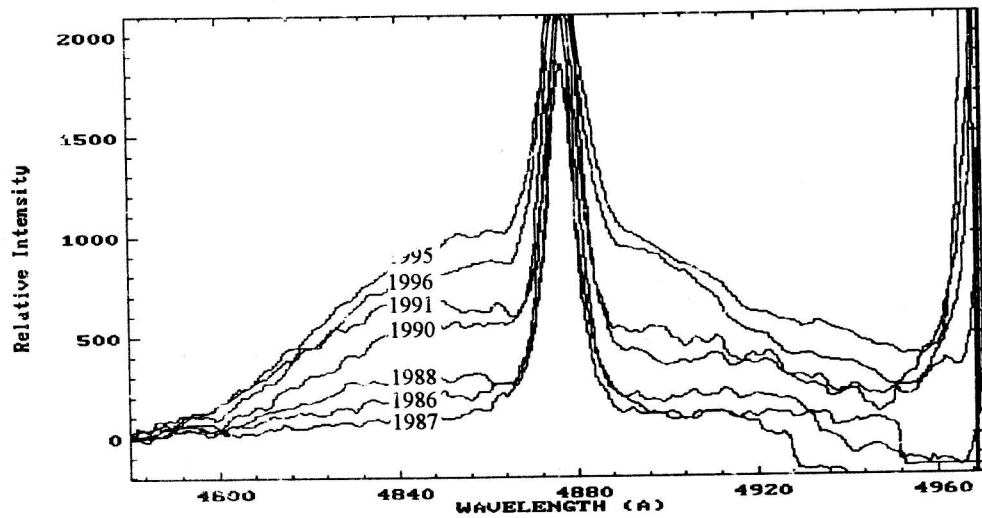


Figure 2: NGC 4151. Average profiles of broad  $H_{\beta}$  for each year.

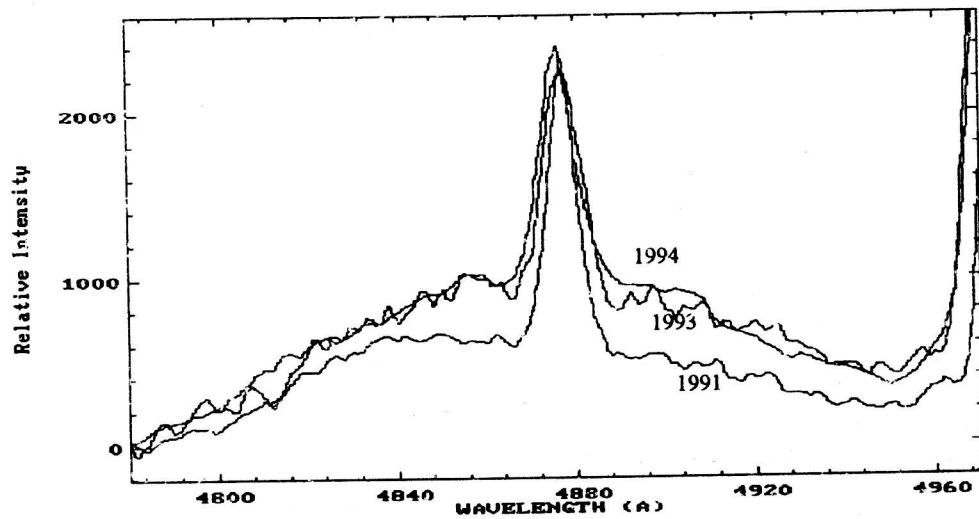


Figure 3: NGC 4151. Average profiles of broad  $H_{\beta}$  for each year.

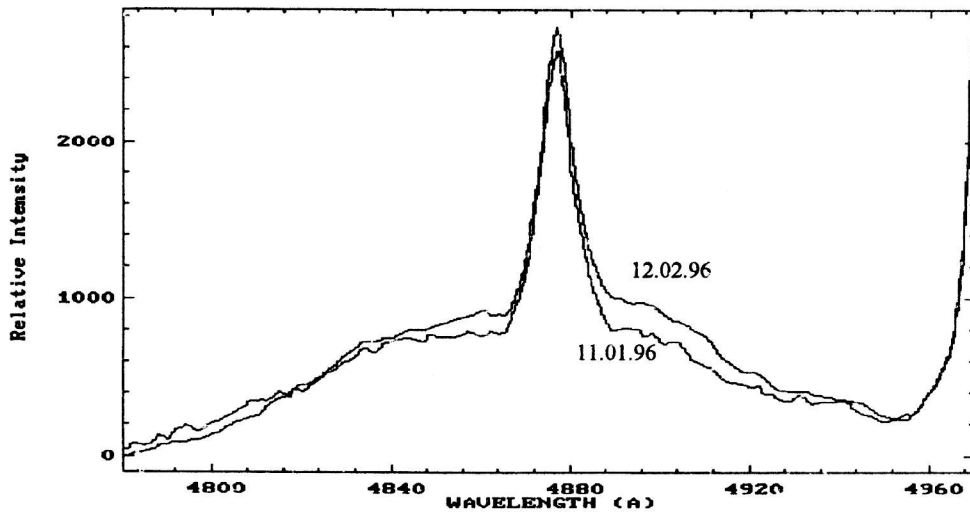


Figure 4: NGC 4151. Two individual profiles of broad  $H\beta$  in 1996.

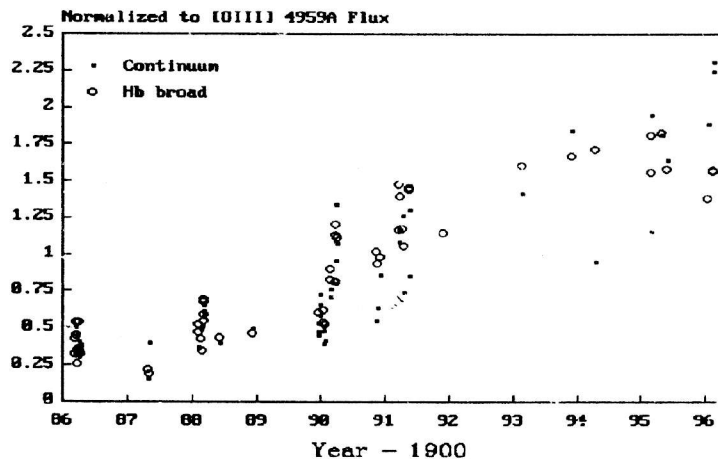


Figure 5: NGC 4151. The data of monitoring in 1986–1996. Average  $\text{flux}(\text{continuum})/\text{flux}([\text{OIII}] \lambda 4959)$  and  $\text{flux}(\text{broad } H\beta)/\text{flux}([\text{OIII}] \lambda 4959)$  for each year. Fluxes are measured within the wavelength range: for continuum —  $\lambda\lambda 4705\text{--}4765 \text{ \AA}$ , broad  $H\beta$  —  $\lambda\lambda 4795\text{--}4930 \text{ \AA}$ .

scope in 1995–96 at 7 different epochs:

- with the UAGS spectrograph and CCD (long slit; 26.04.1995, 17.11.1995, 29.11.95, 30.11.1995; 12.02.1996, 19.03.1996) in the spectral range 3700–5500  $\text{\AA}$  and 4450–7000  $\text{\AA}$  with a resolution of 4  $\text{\AA}$  and 10  $\text{\AA}$ , respectively;

- with the multi-pupil field spectrograph (MPFS; 26.5.95) and CCD. The spectral range and the spectral resolution are 4850–5400  $\text{\AA}$  and 4  $\text{\AA}$ , respectively. An array of  $8 \times 10$  squared microlenses was used. The scale of the image constructed by one lens was  $1''.2 \times 1''.2$ .

2–4 spectra were usually taken on every night in order to have a possibility for correct removal of cos-

mic particles. The spectra taken on one and the same night were summed up and only the summary spectra were analyzed in the apertures  $(2\text{--}3)'' \times (4\text{--}6)''$  (long slit) and  $3''.6 \times 3''.6$  (MPFS). The aperture of integration along the slit depended upon the seeing and was chosen so that practically all the emission from the nucleus is registered. The S/N of the summary spectra in the continuum of  $H\beta$  was usually about 50–100. All the spectra were normalized to the integral flux in  $[\text{OIII}](4959+5007)$ , whose value was adopted equal to  $1.7 \cdot 10^{13} \text{ erg/cm}^2\text{s}$ , according to Veilleux and Zheng (1991). The emission spectra obtained after continuum subtraction were analyzed.

a) **Variability of the broad component of  $H\beta$  and continuum**

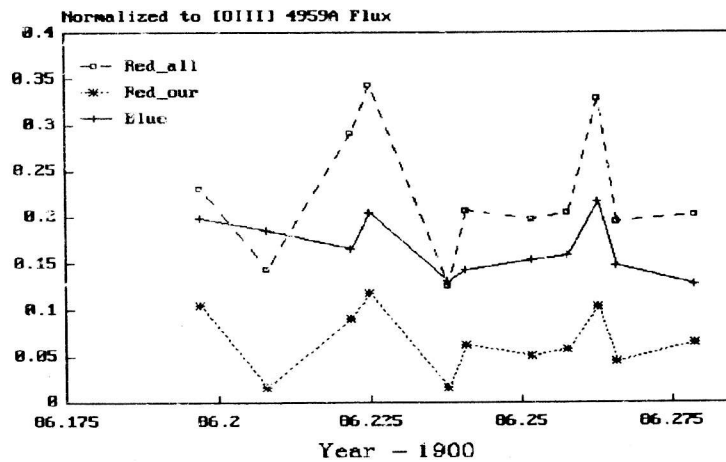


Figure 6: NGC 4151. The data of monitoring in 1986:  $\text{flux}(H_\beta \text{ broad components})/\text{flux}([OIII] \lambda 4959)$ . Flux ratios are measured within the wavelength range: for blue —  $\lambda\lambda 4795\text{--}4857 \text{ \AA}$ , red\_all —  $\lambda\lambda 4857\text{--}4930 \text{ \AA}$ , red\_our —  $\lambda\lambda 4897\text{--}4930 \text{ \AA}$ .

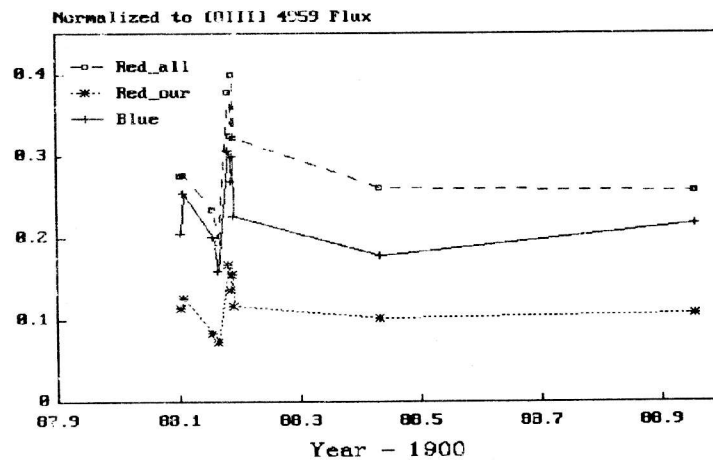


Figure 7: NGC 4151. The data of monitoring in 1988:  $\text{flux}(H_\beta \text{ broad components})/\text{flux}([OIII] \lambda 4959)$ . Flux ratios are measured within the wavelength range: for blue —  $\lambda\lambda 4795\text{--}4857 \text{ \AA}$ , red\_all —  $\lambda\lambda 4857\text{--}4930 \text{ \AA}$ , red\_our —  $\lambda\lambda 4897\text{--}4930 \text{ \AA}$ .

Fig. 14 shows the profiles of the broad component of  $H_\beta$  obtained after subtraction of the narrow component and  $[OIII]4959, 5007$ . It is well seen that the broad component of  $H_\beta$  is characterized by two "bumps" in the blue and red wings at a distance of  $\pm 3500 \text{ km/s}$  from the centre of the narrow component. During the observational run (26.04.1995–19.03.1996) the blue wing was brighter than the red one. For the subsequent quantitative comparison of our results with the bulk of data of Veilleux and Zheng (1991) we measured the observed integral fluxes in  $H_\beta$  line and the flux density in the continuum for the same wavelength intervals.

Our results of continuum and broad  $H_\beta$  component fluxes are presented in Table 1: 1 — observation dates; 2 — JD; 3 — the flux density in continuum in the spectral range  $5100\text{--}5150 \text{ \AA}$ ; 4 — the total integral flux in  $H_\beta$  line (including the narrow component) in the spectral range  $4960\text{--}5340 \text{ \AA}$ ; 5 — the integral flux in the blue wing of  $H_\beta$  in the spectral range  $5020\text{--}5100 \text{ \AA}$ ; 6 — the integral flux in the red wing of  $H_\beta$  in the spectral range  $5150\text{--}5200 \text{ \AA}$ ; 7 — the total integral flux of the broad component of  $H_\beta$  (after removal of the narrow component by Gauss analysis) in the spectral range  $4960\text{--}5340 \text{ \AA}$ .

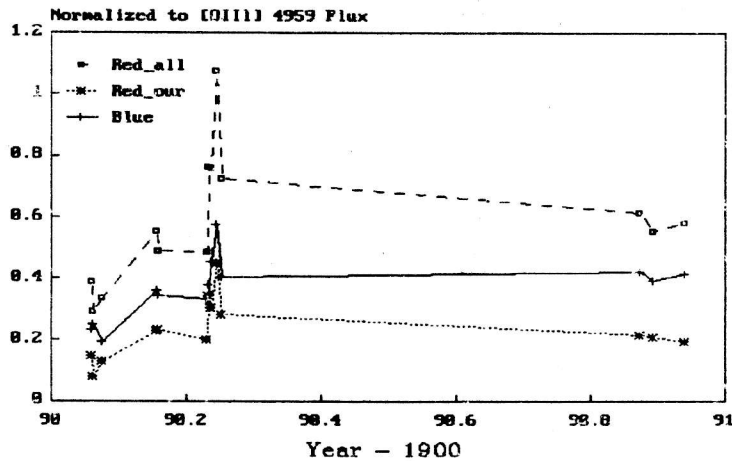


Figure 8: NGC 4151. The data of monitoring in 1990:  $\text{flux}(H_{\beta} \text{ broad components})/\text{flux}([OIII] \lambda 4959)$ . Fluxes are measured within the wavelength range: for blue —  $\lambda\lambda 4795\text{--}4857 \text{ \AA}$ , red\_all —  $\lambda\lambda 4857\text{--}4930 \text{ \AA}$ , red\_our —  $\lambda\lambda 4897\text{--}4930 \text{ \AA}$ .

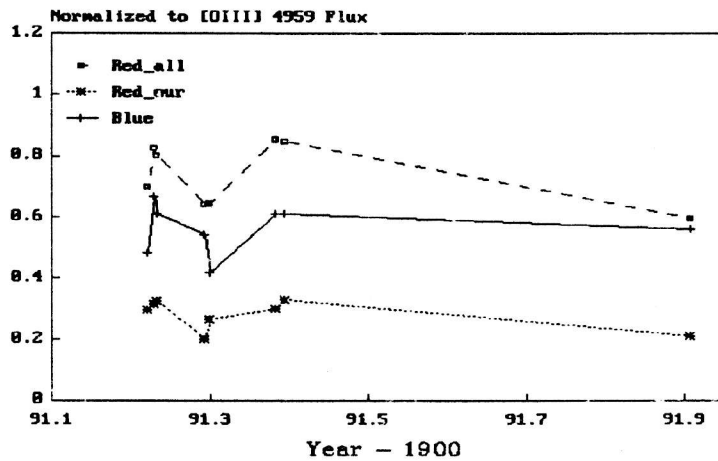


Figure 9: NGC 4151. The data of monitoring in 1991:  $\text{flux}(H_{\beta} \text{ broad components})/\text{flux}([OIII] \lambda 4959)$ . Fluxes are measured within the wavelength range: for blue —  $\lambda\lambda 4795\text{--}4857 \text{ \AA}$ , red\_all —  $\lambda\lambda 4857\text{--}4930 \text{ \AA}$ , red\_our —  $\lambda\lambda 4897\text{--}4930 \text{ \AA}$ .

Fig. 15 presents the flux densities in continuum obtained in 1974–88, which are taken from Veilleux and Zheng (1991), and our results obtained in 1995–96. It is well seen that in 1995–96 the flux density in continuum increased as compared to that of 1974–88. The flux density in continuum in 12.02.1996 (our maximum value) increased two times as compared to the maximum values of 1975 and six times as compared to the minimum of 1980. The integral flux of  $H_{\beta}$  varied in the same manner, but with a lower amplitude (Fig.16).

From Figs. 17 and 18, where only our results of 1995–96 are presented, it follows that the behaviour

of the fluxes in  $H_{\beta}$  line and in continuum differs; the flux density in continuum increased constantly up to the maximum on 12.02.1996 and then it began to fall. The flux intensity of  $H_{\beta}$  in the broad component decreased from 26.05.1995 to 17.11.1995 and then it began to increase but with a higher amplitude than in continuum. On 19.03.1996 the flux in continuum decreased, and in  $H_{\beta}$  line it continued to increase. The different behaviour of the line and continuum fluxes is likely to be indicative of response lag in the lines with respect to the continuum variations. But we cannot determine the value of this lag because of the small density of observations.

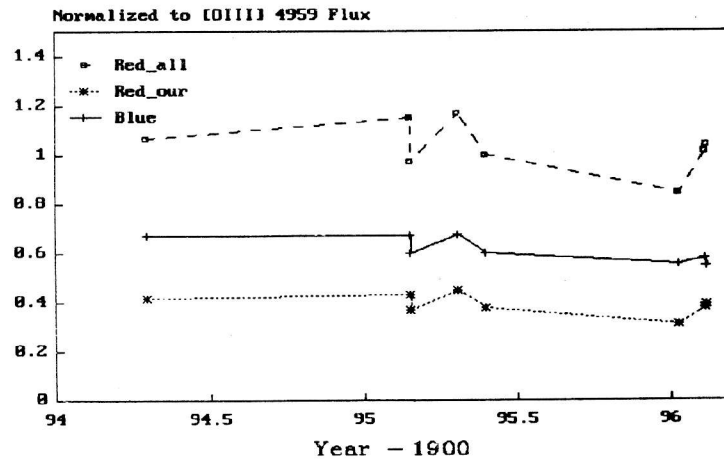


Figure 10: *NGC 4151*. The data of monitoring in 1994–1996:  $\text{flux}(H_{\beta} \text{ broad components})/\text{flux}([OIII] \lambda 4959)$ . Fluxes are measured within the wavelength range: for blue —  $\lambda\lambda 4795\text{--}4857 \text{ \AA}$ , red\_all —  $\lambda\lambda 4857\text{--}4930 \text{ \AA}$ , red\_our —  $\lambda\lambda 4897\text{--}4930 \text{ \AA}$ .

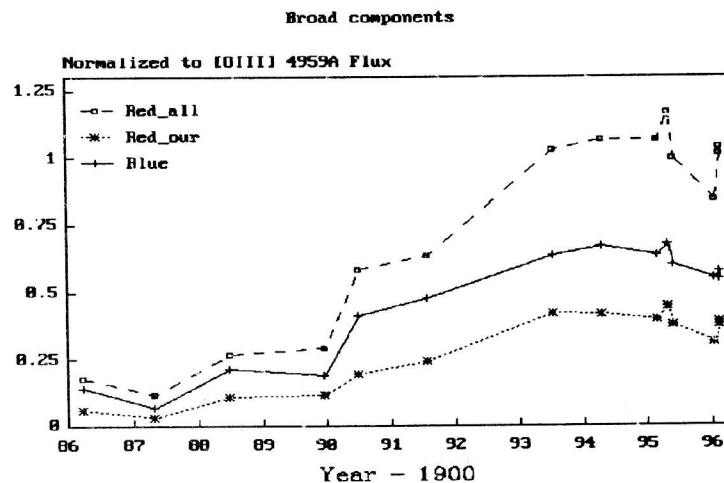


Figure 11: *NGC 4151*. The data of monitoring in 1986–1996. Average  $\text{flux}(H_{\beta} \text{ broad components})/\text{flux}([OIII] \lambda 4959)$  for each year. Fluxes are measured within the wavelength range: for blue —  $\lambda\lambda 4795\text{--}4857 \text{ \AA}$ , red\_all —  $\lambda\lambda 4857\text{--}4930 \text{ \AA}$ , red\_our —  $\lambda\lambda 4897\text{--}4930 \text{ \AA}$ .

#### b) The blue and red wings of broad $H_{\beta}$

Figs. 19 and 20 show the behaviour of the fluxes in the blue and red wings and their ratios in 1974–88 (Veilleux and Zheng, 1991) and in 1995–96 (our measurements).

The flux intensities in the wings increased in 1995–96 as well as the whole broad component of  $H_{\beta}$ , and the flux in the blue wing was always more intensive than in the red one. The flux ratios in the blue and red wings are close to the values, obtained by Veilleux and Zheng (1991) in 1975, 1985. These values follow well the periodical ( $\sim 10$  years) sinusoidal dependence for the flux ratios in the blue and red wings of  $H_{\beta}$ ,

obtained by Veilleux and Zheng (1991), and correspond approximately to the sinusoid maximum. Our measurements of the flux densities in the wings and their ratios are shown in Figs. 21 and 22. In November 1995 – February 1996 the flux variability in the blue wing was twice as intensive as that in the red one. From Fig. 22 it follows that the fluxes in the wings vary almost quasimultaneously. This is an indication of the absence of considerable radial motions in the BLR 3C390.3.

This research is supported by a grant from the Russian Foundation of Fundamental Research 94–02–4885a.

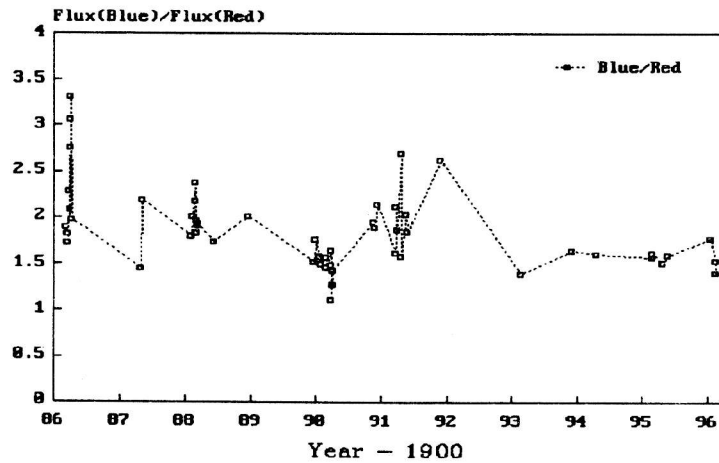


Figure 12: NGC 4151. The data of monitoring in 1986–1996:  $\text{flux}(H_{\beta} \text{ blue component})/\text{flux}(\text{red component } H_{\beta})$ . Fluxes are measured within the wavelength range: for blue —  $\lambda\lambda 4795\text{--}4857 \text{ \AA}$ , red —  $\lambda\lambda 4897\text{--}4930 \text{ \AA}$ .

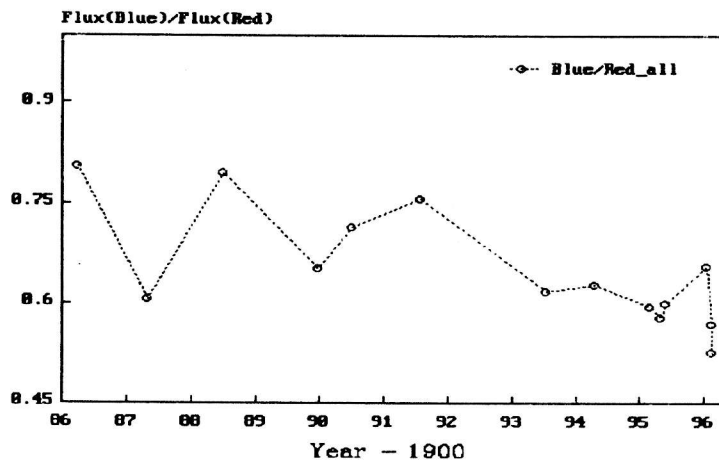


Figure 13: NGC 4151. The data of monitoring in 1986–1996. Average  $\text{flux}(H_{\beta} \text{ blue component})/\text{flux}(\text{red component } H_{\beta})$  for each year. Fluxes are measured within the wavelength range: for blue —  $\lambda\lambda 4795\text{--}4857 \text{ \AA}$ , red —  $\lambda\lambda 4857\text{--}4930 \text{ \AA}$ .

## References

- Bochkarev N.G., Antokhin I.I.: 1982, *Soviet Astron.*, **27**, 261.
- Maoz D., Netzer H., Mazeh T., Beck S., Almozino E., Leibowitz E., Brosch N., Mendelson H., and Laor A.: 1991, *Astrophys. J.*, **367**, 493.
- Veilleux S., Zheng W.: 1991, *Astrophys. J.*, **377**, 89.



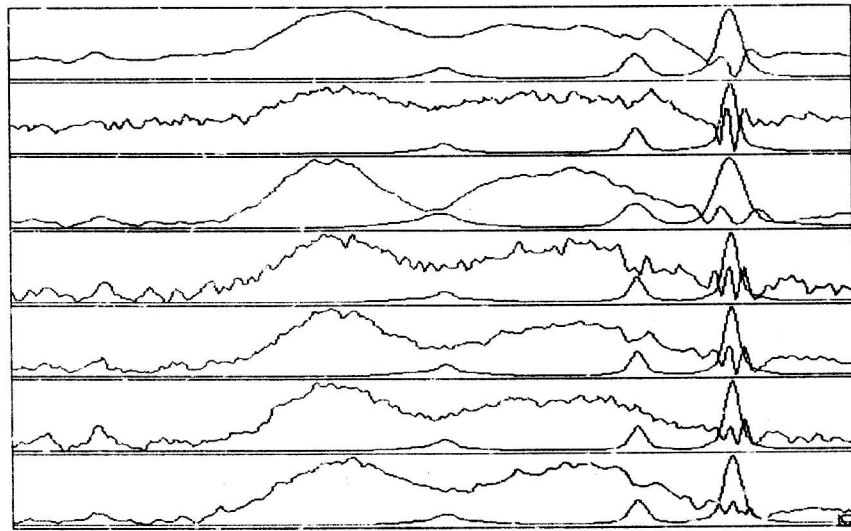


Figure 14: 3C390.3. Broad components after subtraction of the narrow component of  $H\beta$  and  $[OIII]$  and profiles of narrow  $H\beta$  and  $[OIII]$  approximation by Gaussians. Spectra for (JD-2440000): 9833, 9864, 10039, 10052, 10127, 10163 are presented from top to bottom in the range  $\lambda\lambda$  4900-5350  $\text{\AA}$ .

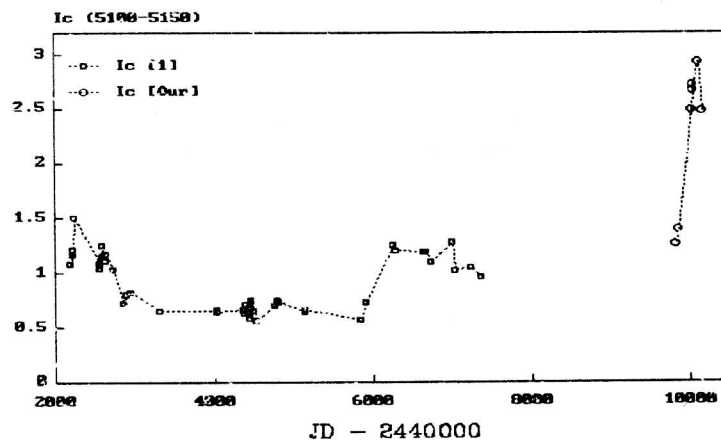


Figure 15: 3C390.3. The data of monitoring in 1974-1996, ([1] — from Veilleux and Zheng, 1991; and our for 1995-1996). Flux density in continuum is in  $10^{-15} \text{erg s}^{-1} \text{cm}^{-2} \text{\AA}^{-1}$ . It is measured within the wavelength range  $\lambda\lambda$  5100-5150  $\text{\AA}$ .

Table 1: Results of flux measurements for 3C390.3.

Date	Julian Date JD-2440000	$I_{Cont}$ 5100-5150 Å	$F_{Total H\beta}$ 4960-5340 Å	$F_{Broad H\beta}$ 4960-5340 Å	$F_{Blue}$ 5020-5100 Å	$F_{Red}$ 5150-5200 Å
25.04.1995	9833.4	1.26	1.34	1.08	4.08	2.55
26.05.1995	9864.4	1.39	1.59	1.33	4.39	2.96
17.11.1995	10039.2	2.49	1.49	1.04	4.39	3.12
29.11.1995	10051.1	2.67	1.81	1.37	4.95	3.54
30.11.1995	10052.1	2.72	1.92	1.46	5.48	3.57
12.02.1996	10126.6	2.93	2.09	1.68	6.24	3.99
19.03.1996	10162.6	2.48	2.14	1.75	5.83	4.30

The unit of  $I_{cont}$  is  $10^{-15} \text{ ergs s}^{-1} \text{ cm}^{-2} \text{ \AA}^{-1}$ . The units of  $F_{Total H\beta}$  and  $F_{Broad H\beta}$  are  $10^{-13} \text{ ergs s}^{-1} \text{ cm}^{-2}$ . The units of  $F_{Blue}$  and  $F_{Red}$  are  $10^{-14} \text{ ergs s}^{-1} \text{ cm}^{-2}$ .

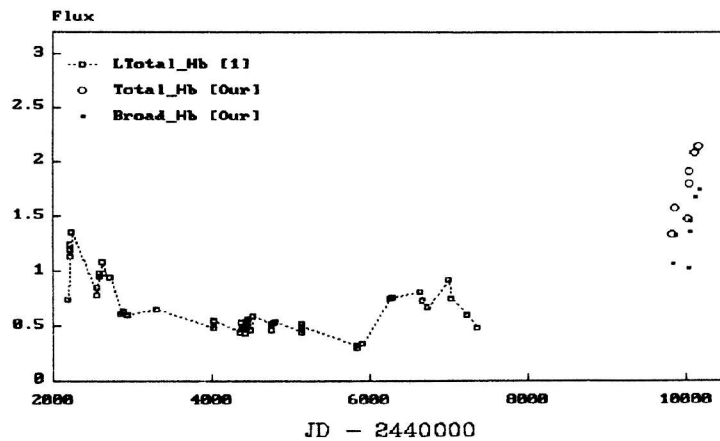


Figure 16: 3C390.3. The data of monitoring in 1974-1996, ([1] — from Veilleux and Zheng, 1991; and ours for 1995-1996). Total  $H\beta$  and broad components only. Fluxes are in  $10^{-13} \text{ erg s}^{-1} \text{ cm}^{-2}$ . Fluxes: Broad\_ $H\beta$  and Total\_ $H\beta$  (as well as LTotal\_ $H\beta$ ) are measured within the wavelength range  $\lambda\lambda$  4960-5340 Å.

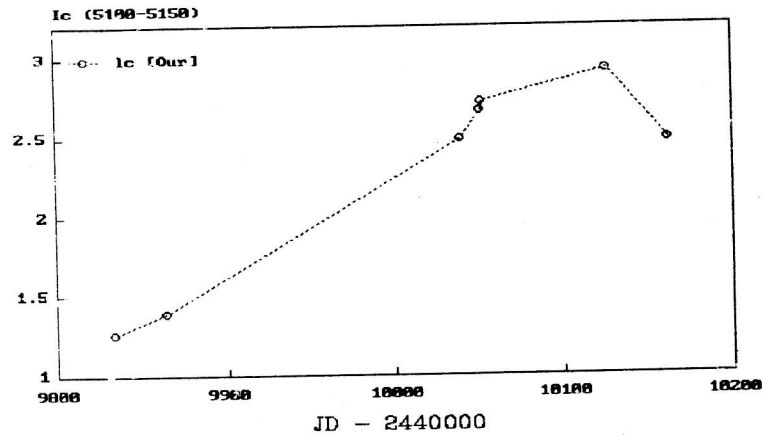


Figure 17: 3C390.3. The data of monitoring in 1995-1996. Flux density in continuum is  $10^{-15} \text{erg s}^{-1} \text{cm}^{-2} \text{\AA}^{-1}$ . It is measured within the wavelength range  $\lambda \lambda 5100 - 5150 \text{\AA}$ .

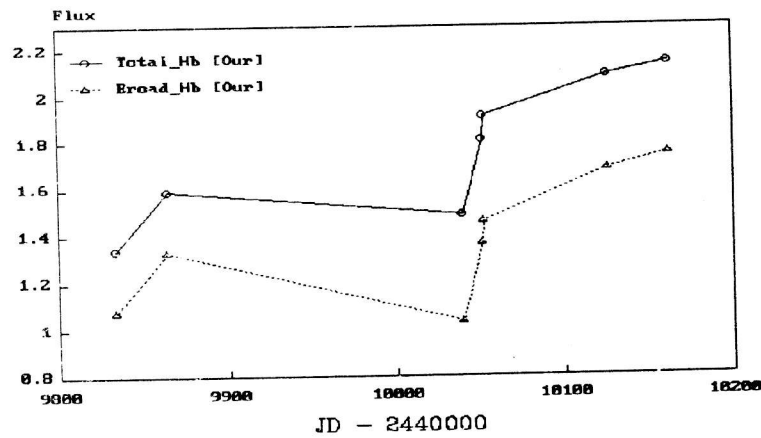


Figure 18: 3C390.3. The data of monitoring in 1995-1996. Total  $H\beta$  and broad components only. Fluxes: Broad\_ $H\beta$  and Total\_ $H\beta$  (as well as  $L_{\text{Total}_H\beta}$ ) are measured within the wavelength range  $\lambda \lambda 4960 - 5340 \text{\AA}$ .

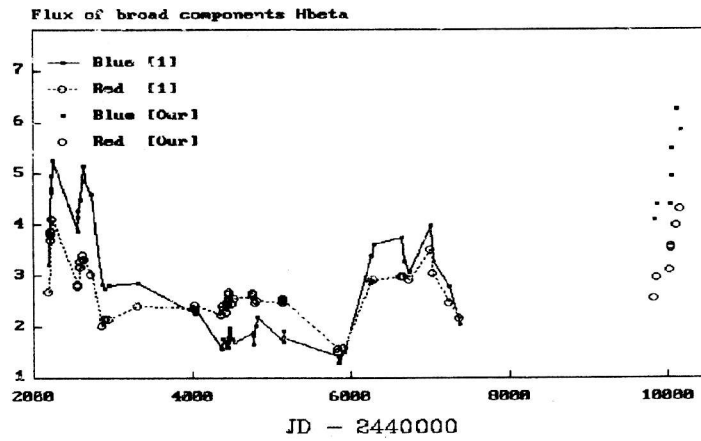


Figure 19: 3C390.3. The data of monitoring in 1974–1996, ([1] — from Veilleux and Zheng, 1991; and ours for 1995–1996). Fluxes of broad blue and red components of  $H\beta$  are in  $10^{-14} \text{erg s}^{-1} \text{cm}^{-2}$ . Fluxes are measured within the wavelength range: for blue —  $\lambda\lambda 5020\text{--}5100 \text{ \AA}$  and red —  $\lambda\lambda 5150\text{--}5200 \text{ \AA}$ .

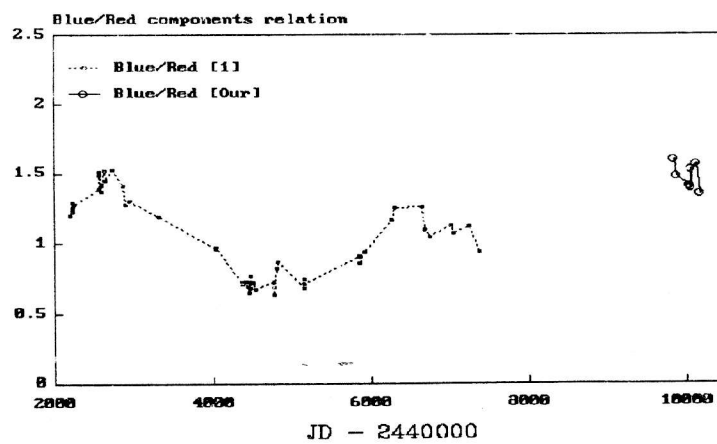


Figure 20: 3C390.3. The data of monitoring in 1974–1996, ([1] — from Veilleux and Zheng, 1991; and ours for 1995–1996). Relation of blue/red components of  $H\beta$  is given.

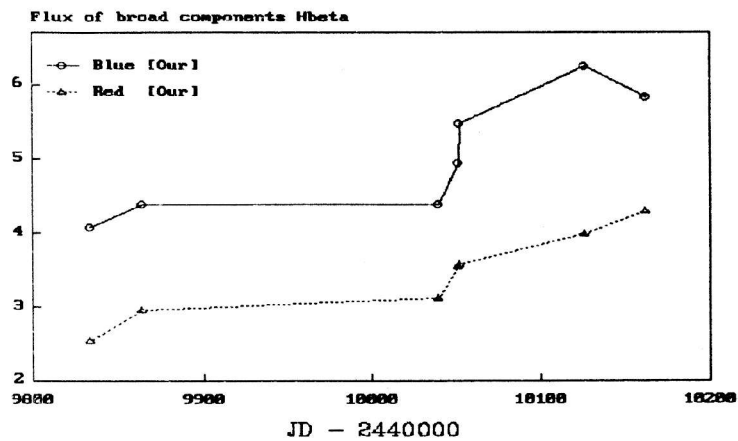


Figure 21: *3C390.3*. The data of monitoring in 1995–1996. Fluxes of broad blue and red components of  $H_{\beta}$  in  $10^{-14} \text{erg s}^{-1} \text{cm}^{-2}$ . Fluxes are measured within the wavelength range: for blue —  $\lambda\lambda 5020\text{--}5100 \text{ \AA}$  red —  $\lambda\lambda 5150\text{--}5200 \text{ \AA}$ .

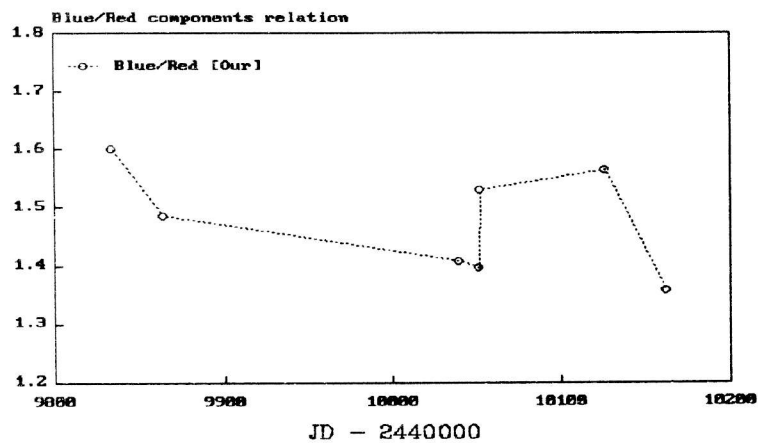


Figure 22: *3C390.3*. The data of monitoring in 1995–1996. Relation of blue/red components of  $H_{\beta}$  is given.